Research Paper

Experimental Physiology

Characterization of the anisotropic mechanical behaviour of colonic tissues: experimental activity and constitutive formulation

E. L. Carniel[1,2], V. Gramigna[4], C. G. Fontanella[2], A. Frigo[1,2], C. Stefanini[4], A. Rubini[2,3] and A. N. Natali[1,2]

[1]*Department of Industrial Engineering,* [2]*Centre of Mechanics of Biological Materials and* [4]*Department of Biomedical Sciences, University of Padova, Padova, Italy*
[3]*The BioRobotics Institute, Scuola Superiore Sant'Anna, Pisa, Italy*

New Findings

- **What is the central question of this study?**
  The wall of the colon shows an anisotropic and non-linear mechanical response, because of the distribution and mechanical properties of sub-components. This study aimed to provide, by a coupled experimental and computational approach, a constitutive framework to interpret the mechanics of colonic tissues.
- **What is the main finding and its importance?**
  Tensile tests on tissue samples from pig colon were developed. The experimental data were processed to define proper constitutive formulations. Constitutive parameters were identified by the inverse analysis of experimental tests. The reliability of parameters was assessed by agreement between the experimental and model results and the satisfaction of material thermomechanics principles. The developed constitutive framework is capable of interpreting the general anisotropic and non-linear mechanical behaviour of colonic tissues.

The aim was to investigate the biomechanical behaviour of colonic tissues by a coupled experimental and numerical approach. The wall of the colon is composed of different tissue layers. Within each layer, different fibre families are distributed according to specific spatial orientations, which lead to a strongly anisotropic configuration. Accounting for the complex histology of the tissues, mechanical tests must be planned and designed to evaluate the behaviour of the colonic wall in different directions. Uni-axial tensile tests were performed on tissue specimens from 15 fresh pig colons, accounting for six different loading directions (five specimens for each loading direction). The next step of the investigation was to define an appropriate constitutive framework and develop a procedure for identification of the constitutive parameters. A specific hyperelastic formulation was developed that accounted for the multilayered conformation of the colonic wall and the fibre-reinforced configuration of the tissues. The parameters were identified by inverse analyses of the mechanical tests. The comparison of model results with experimental data, together with the evaluation of satisfaction of material thermomechanics principles, confirmed the reliability of the analysis developed. This work forms the basis for more comprehensive activities that aim to provide computational tools for the interpretation of surgical procedures that involve the gastrointestinal tract, considering the specific biomedical devices adopted.

(Received 30 August 2013; accepted after revision 27 January 2014; first published online 31 January 2014)
Corresponding author E. L. Carniel: Department of Industrial Engineering, Centre of Mechanics of Biological Materials, University of Padova, Via G. Colombo 3, I-35131 Padova, Italy. Email: emanueleluigi.carniel@unipd.it

 DOI: 10.1113/expphysiol.2013.076091

Introduction

Computational methods are frequently applied for the investigation of the mechanical behaviour of biological tissues and structures, with particular regard to the analysis of interaction phenomena between biological tissues and biomedical devices (Tillier *et al.* 2003; Lapeer *et al.* 2010; Böhme *et al.* 2012; Owida *et al.* 2012). Computational models of gastrointestinal organs and structures can be developed to analyse the response of the tissues in terms of stress and strain, for evaluating the reliability of endoscopic and surgical devices (Ciarletta *et al.* 2009; Liao *et al.* 2009; Bellini *et al.* 2011; Nováček *et al.* 2012). The development of such computational models requires the definition of constitutive formulations of the biological tissues (Maurel *et al.* 1998; Natali *et al.* 2009). The studies proposed here aim to provide a reliable constitutive framework for the mechanical characterization of colonic tissues. The preliminary activity of the constitutive analysis pertains to the investigation of the tissue histology. The action entails the evaluation of the structural conformation of the material and the planning of the mechanical tests that must be performed to provide a comprehensive characterization of the tissue mechanics. The experimental data, comprising the results from the histological investigation and the mechanical tests, must be processed to provide the constitutive formulation, which is defined in the framework of the axiomatic theory of constitutive relationships (Holzapfel, 2000*b*). The next step pertains to the identification of the constitutive parameters, which is performed by the inverse analysis of mechanical tests. Finally, the reliability of the constitutive model and parameters must be assessed by the analysis of further experimental situations, by comparison of model and experimental results, and the evaluation of satisfaction of the principles of materials thermomechanics (Schröder *et al.* 2005).

The colon is a portion of the large bowel, and its wall consists of the four main layers of the gastrointestinal organs, namely the mucosa, submucosa, muscularis externa and serosa. The mucosal layer is mainly composed of epithelial cells and a loose network of collagen fibrils. The submucosa is mainly composed of collagen fibres that are arranged according to two main helixes, a clockwise and an anticlockwise one, which run down the colonic structure. The muscularis externa is mainly composed of smooth muscular fibres that are distributed along the longitudinal and circumferential directions. The longitudinal fibres congregate in three thick bands, known as the taeniae coli, which are equally spaced around the colonic structure. Between these bands, the longitudinal fibres form a thin sheet. Finally, the serosa forms a thin layer composed of loose connective tissue and a squamous epithelium that lines the overall tubular structure (Gabella, 1987; Skinner & O'Brien, 1996; Ge *et al.* 1998; Hidović-Rowe & Claridge, 2005; Huang *et al.* 2004; Junqueira *et al.* 2005).

As a result of its hierarchical and complex configuration, the colonic wall shows anisotropic and strongly non-linear mechanical responses, given by the subcomponents distribution and mechanical properties (Natali *et al.* 2009; Lapeer *et al.* 2010). The arrangement of fibrous elements along preferential directions, in particular with regard to the submucosa and muscularis externa (Fig. 1), entails anisotropic behaviour (Spencer, 1984; Holzapfel, 2000*a*). Rearrangement phenomena, such as the uncrimping and alignment of fibres, reversible sliding of adjacent layers, fluid fluxes, etc., develop within the tissues during loading. Such microstructural processes lead to a progressive variation of the material stiffness with stretch and the resulting non-linearity of the stress–stretch response (Maurel *et al.* 1998). The characterization of such a complex mechanical behaviour requires the development of mechanical tests according to different loading conditions and directions (Egorov *et al.* 2002; Yang *et al.* 2006).

Uni-axial tensile tests were performed on tissue specimens from pig colon, which were harvested along different directions. A specific hyperelastic model was provided to interpret the colon wall mechanics. The model was developed in the framework of the theory of composite materials, accounting for the contributions of the different tissue layers and fibre families (Natali *et al.* 2009). The constitutive parameters were identified, providing a procedure that requires the analysis of the performed mechanical tests and the minimization of discrepancy between model and experimental results (Natali *et al.* 2008, 2011; Forestiero *et al.* 2014). Once the constitutive parameters had been identified, further experimental data were compared with model results to assess the reliability of the model and parameters. The trends of tangent elasticity constants, i.e. the tangent Young modulus and the tangent Poisson ratios, were computed to verify the thermomechanical consistency of the formulation and the parameters (Lempriere, 1968; Schröder *et al.* 2005; Scott, 2007).

Methods

Experimental tests

The experimental tests were performed on tissue specimens from pig colon, because of the extensively supported similarity of pig and human tissue mechanics. Experimental tests were developed following a procedure similar to the one proposed by Yang *et al.* (2006) for the mechanical characterization of oesophageal tissues. Fresh transverse colons from 15 Large White pigs (11–13 months old and weighing ∼130 kg) were obtained from a local abattoir. After excision of a colonic segment, it was cleaned of luminal contents, the adjacent tissues were dissected, and the segment was cut longitudinally and straightened on a Teflon plate. Tissue specimens were dissected according to a rectangular shape (length, 60 mm and width, 10 mm). Specimens included tissues from the haustra only and were prepared by isolating regions of the colonic wall between adjacent taeniae coli strands. Five specimens for each of the different cutting directions, i.e. 0, 15, 30, 45, 60 and 90 deg with respect to the circumferential direction, were prepared. Callipers were used to measure the tissue thickness at different positions within each specimen, and the specific mean values, which were ~2.5 mm, were considered for the computation of the specific reference cross-sectional areas of the different specimens. Colon structures and tissue specimens were stored in or dampened with physiological saline (0.9% NaCl) at room temperature during preparation. Mechanical tests were performed within 6 h after the slaughter of the animals.

An Instron 4464 machine was used to perform tensile tests up to failure of the tissue specimens. Following preliminary evaluation of the strength of samples, a load cell with a capacity of 100 N and accuracy of ±0.1% was adopted. Further preliminary tests were performed to evaluate the influence of strain rate on viscous effects. The results showed that a strain rate of 40% s^{-1} minimizes the influence of viscous phenomena and prevents the dynamic effects that may develop when higher strain rates are adopted (Fung, 1993; Weiss & Gardiner, 2001). According to the imposed strain rate, the force was recorded with a frequency of 10 Hz.

Clamping of the specimens was performed using grips (5 mm in length and 20 mm wide), at a pressure of ~100 kPa. The pressure was adjusted to avoid slippage and damage of the specimens. The clamping apparatus was designed to keep the experimental sample within a glass beaker filled with physiological saline (0.9% NaCl). A thermal bench was provided under the beaker to maintain the temperature constant at 39 ± 2°C, which is the typical temperature of healthy pigs.

The major difference between the experimental tests performed here and the common soft-tissue biomechanical testing pertains to tissue preconditioning. Due to the typical properties of soft tissues, their mechanical response changes with each successive loading cycle (Fung, 1993). A stable behaviour can develop after several loading cycles. Preconditioning a tissue before testing takes about 10–20 cycles. As gastrointestinal tissues are not preconditioned before surgery, the first-cycle behaviour is of great interest. The aim of the present experiments was to characterize colonic tissue mechanics during endoscopy or surgery; therefore, no preconditioning was performed (Rosen *et al.* 2008).

The conformation of the stress and stretch fields during uni-axial testing was preliminarily investigated by finite element analyses using the general-purpose code Abaqus 6.8 (Dassault Systèmes Simulia Corp., Providence, RI, USA). A simplified constitutive formulation, known

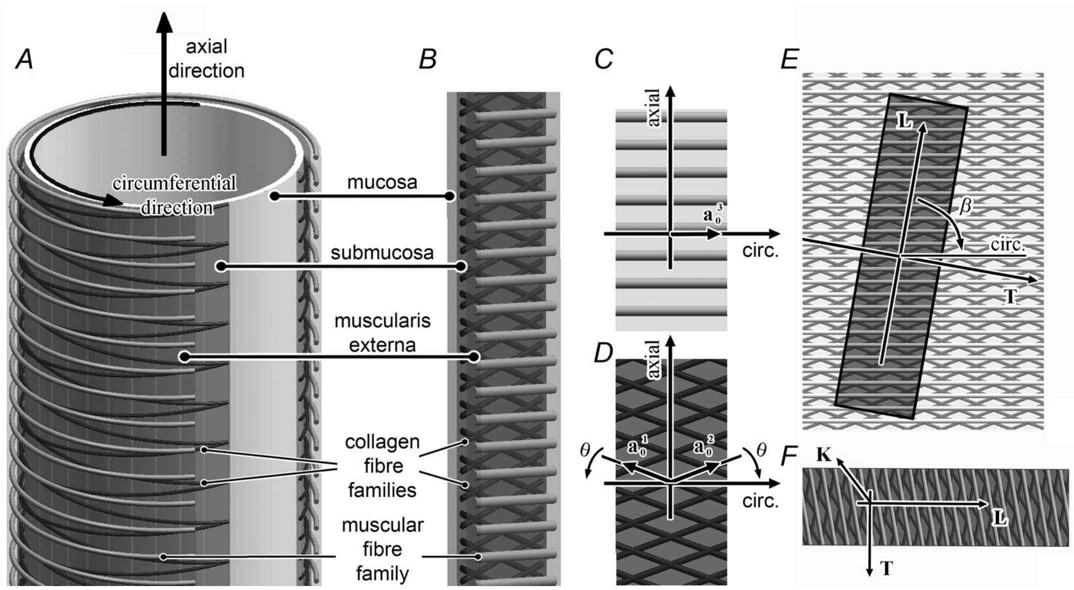

Figure 1. Conformation of colonic tissues
Schematic representation of distribution of tissues and tissue subcomponents within the colonic wall (*A* and *B*). Definition of fibre orientations and unit vectors with regard to the muscularis externa (*C*) and submucosa (*D*). Localization of tensile specimens within the colonic wall (*E*) and definition of the experimental reference system LTK (*F*).

as the neo-Hookean hyperelastic model, was assumed to characterize the tissue mechanics. The assumption is admissible because the numerical analyses were performed only for a preliminary evaluation of the stress and strain distribution within the specimen. The results of the analyses demonstrated the presence of an almost homogeneous stretch and stress field within a central region of the specimen, whose length was about 30 mm. A region 30 mm in length was consequently assumed for the experimental evaluation of stretch components.

Video image analysis techniques were adopted to monitor the shape evolution of this central region, leading to the evaluation of stretches in the loading and transverse directions, along the specimen length and width, respectively. On the central region of each tissue specimen, five pairs of marks were drawn, placed at regular distances of 6 mm from each other, along the specimen length. The evolution of the shape of the region during the tensile test was recorded by a digital video camera (Sony Handycam, DCR-SR57E). Video tracks were analysed by automatic tracking with the ProAnalyst Suite software (Xcitex Inc., Cambridge, MA, USA). The video-tracking methodology was based on the determination of the frame-by-frame position of the marks over time (Shrive, 1996; Hung & Voloshin, 2003). The loading stretch was computed by analysing the relative motion along the loading direction of the mid-points of the first and the fifth pairs of marks. The transverse stretch was evaluated by averaging the relative motions along the width of the specimen of the marks in each pair. Nominal stress was computed as the ratio between the force and the reference cross-sectional area of the specimen.

The results from tensile tests on the different specimens were postprocessed. Each nominal stress–loading stretch curve was characterized by the typical trend of soft biological tissue mechanics, showing an initial low stiffness that progressively increased with stretch up to a maximal value (Fung, 1993). When the loading was increased further, damage phenomena took place and tissue stiffness decreased with a typical softening trend (Natali *et al.* 2008). Within our proposed hyperelastic formulation of colonic tissues, experimental data pertaining to the damage region were discarded. With regard to each experimental loading direction, the overall nominal stress–loading stretch and the transverse stretch–loading stretch data were preliminarily fitted by specific exponential and power functions, respectively (Natali *et al.* 2009). This procedure made it possible to provide average nominal stress–loading stretch and transverse stretch–loading stretch curves. The statistical analysis of the distribution of the experimental data around the average curves entailed the definition of scatter bands, which identified the domains of reliable experimental results.

Hyperelastic formulation

The mechanical response of the wall of the colon was interpreted by using a hyperelastic constitutive formulation. The model must account for mechanical contributions from the different layers, with particular regard to the mucosa, submucosa and muscularis externa (Yang *et al.* 2006; Natali *et al.* 2009). The mucosa is characterized by isotropic behaviour because of the random distribution of collagen fibrils. In contrast, the preferential orientations of fibrous elements within the submucosa and muscularis externa determine the overall anisotropic response. The hyperelastic formulation was provided in the framework of fibre-reinforced composite materials theory (Spencer, 1984; Holzapfel, 2000*a*,*b*; Gasser *et al.* 2006).

In detail, two main sets of collagen fibres can be identified in the submucosa (Fig. 1*D*), arranged according to clockwise and anticlockwise helixes (Gabella, 1987), while one family of muscular fibres can be assumed for muscolaris externa (Fig. 1*C*) along the circumferential direction (Ross *et al.* 2010). The local orientation of the *i*th family of fibres is usually defined by the unit vector field, $\mathbf{a}_0^i$. The definition of the strain energy function has to account for the contributions of the different components of the tissue, as a common ground matrix and the three fibre families (Holzapfel, 2000*b*), as follows:

$$W(\mathbf{C}) = W_m(\mathbf{C}) + \sum_{i=1}^{3} W_f^i\left(\mathbf{C}, \mathbf{a}_0^i \otimes \mathbf{a}_0^i\right) + \sum_{i,j=1}^{3} W_f^{ij}\left(\mathbf{C}, \mathbf{a}_0^i \otimes \mathbf{a}_0^j\right) \quad (1)$$

where $\mathbf{C}$ is the right Cauchy-Green strain tensor, W_m is the strain energy of the ground matrix, W_f^i is the contribution of the *i*th family of fibres, while the term W_f^{ij} pertains to interaction phenomena between the *i*th and the *j*th fibre families. The specific formulations of the strain energy contributions were developed by the improvement of a model that has already proved its reliability in the analysis of gastrointestinal tissues mechanics (Natali *et al.* 2009), where the following main terms must be considered:

$$W_m(\mathbf{C}) = U_m(J) + \tilde{W}_m(\tilde{I}_1) \quad (2)$$

$$U_m(J) = \frac{K_v}{2 + r(r+1)}\left[(J-1)^2 + J^{-r} + rJ - (r+1)\right] \quad (3)$$

$$\tilde{W}_m(\tilde{I}_1) = [C_1/\alpha_1]\{\exp[\alpha_1(\tilde{I}_1 - 3)] - 1\} \quad (4)$$

The ground matrix contribution was split into volumetric and isovolumetric terms, as U_m and $\tilde{W}_m$, because of the almost incompressible behaviour of soft biological tissues. The parameter J is the deformation Jacobian and $\tilde{I}_1$ is the first invariant of the isovolumetric part of the right Cauchy-Green strain tensor, i.e. $\tilde{\mathbf{C}} = J^{-2/3}\mathbf{C}$. The constitutive parameters K_v and r characterize the matrix compressibility, while C_1 and α_1 specify the shear behaviour. The fibre contributions were provided by exponential formulations, because of the typical stiffening behaviour of biological fibrous elements, given by:

$$W_f^i\left(\mathbf{C}, \mathbf{a}_0^i \otimes \mathbf{a}_0^i\right) = W_f^i\left(I_4^i\right) = \left[C_4^i/\left(\alpha_4^i\right)^2\right] \times \left\{\exp\left[\alpha_4^i\left(I_4^i - 1\right)\right] - \alpha_4^i\left(I_4^i - 1\right) - 1\right\} \quad (5)$$

The structural invariant $I_4^i = \mathbf{C} : (\mathbf{a}_0^i \otimes \mathbf{a}_0^i) = (\lambda_a^i)^2$ depends on the tissue stretch along fibre direction $\mathbf{a}_0^i$, as λ_a^i, the parameter C_4^i is related to the initial stiffness of the ith fibre family, while α_4^i specifies the increase of fibre stiffness with stretch. When different fibre families reinforce the ground matrix, interaction phenomena between pairs of families must be accounted for by specific strain energy contributions, as follows:

$$W_f^{ij}\left(\mathbf{C}, \mathbf{a}_0^i \otimes \mathbf{a}_0^j\right) = W_f^{ij}\left(I_8^{ij}, I_9^{ij}\right) = C_{89}^{ij}\left[I_8^{ij} - I_9^{ij}\right]^2 \quad (6)$$

The eighth and the ninth invariants, namely $I_8^{ij} = (\mathbf{a}_0^i \cdot \mathbf{a}_0^j)[\mathbf{C} : (\mathbf{a}_0^i \otimes \mathbf{a}_0^j)]$ and $I_9 = (\mathbf{a}_0^i \cdot \mathbf{a}_0^j)^2$, are related to the angle formed by the ith and the jth fibre families in the strained and unstrained configurations, respectively, and the parameter C_{89}^{ij} specifies an angular stiffness (Holzapfel, 2000*b*). From a mechanical point of view, the interaction term is influential when the two families of fibres intertwine with each other, as the two collagen helixes do within the submucosa. Interactions are less relevant when fibre families belong to different planes or layers, such as the muscular fibres of the muscularis externa and the collagen fibres of the submucosa, and the associated strain energy contributions can be neglected (Holzapfel, 2000*a*).

Identification of constitutive parameters

Parameters were evaluated by analysis of data from tensile tests developed along four different loading directions, namely 0, 30, 60 and 90 deg, and accounting for the trends of both nominal stress and transverse stretch in relationship to the loading stretch. The further experimental results, i.e. the data from the tests along 15 and 45 deg directions, were later processed to assess the reliability of parameters.

A fitting procedure was applied to minimize the discrepancy between model and experimental results (Natali *et al.* 2008, 2011; Forestiero *et al.* 2014). The first step of the procedure pertains to the development of predictive models to interpret the experimental tests, accounting for the constitutive formulation and the specific boundary conditions. With regard to uni-axial tensile tests, the predictive model has to provide a relationship between the nominal stress along the loading direction and the corresponding strain configuration. For a hyperelastic material, the general stress–strain relationship is evaluated as $\mathbf{P} = 2\mathbf{F}\partial W/\partial\mathbf{C}$, where $\mathbf{P}$ is the first Piola–Kirchhoff stress tensor, a measure of nominal stress, and $\mathbf{F}$ is the deformation gradient (Holzapfel, 2000*b*). Accounting for the proposed formulation of the strain energy function, the first Piola–Kirchhoff stress tensor was defined as follows:

$$\mathbf{P} = \bar{\mathbf{P}}_m + \tilde{\mathbf{P}}_m + \sum_{i=1}^{n}\mathbf{P}_f^i + \sum_{i,j=1}^{n}\mathbf{P}_f^{ij} \quad (7)$$

$$\bar{\mathbf{P}}_m = 2\mathbf{F}\partial U_m/\partial\mathbf{C} = [K_v/2 + r(r+1)] \times [2J(J-1) - rJ^{-r} + rJ]\mathbf{F}^{-T} \quad (8)$$

$$\tilde{\mathbf{P}}_m = 2\mathbf{F}\partial\tilde{W}_m/\partial\mathbf{C} = C_1\exp[\alpha_1(\tilde{I}_1 - 3)] \times (2J^{-2/3}\mathbf{F} - 2/3\tilde{I}_1\mathbf{F}^{-T}) \quad (9)$$

$$\mathbf{P}_f^i = 2\mathbf{F}\partial W_f^i/\partial\mathbf{C} = 2\left(C_4^i/\alpha_4^i\right)\left\{\exp\left[\alpha_4^i\left(I_4^i - 1\right)\right] - 1\right\} \times \mathbf{F}\left(\mathbf{a}_0^i \otimes \mathbf{a}_0^i\right) \quad (10)$$

$$\mathbf{P}_f^{ij} = 2\mathbf{F}\partial W_f^{ij}/\partial\mathbf{C} = C_{89}^{ij}\left[I_8^{ij} - I_9^{ij}\right]\left(I_9^{ij}\right)^{1/2} \times \mathbf{F}\left(\mathbf{a}_0^i \otimes \mathbf{a}_0^j + \mathbf{a}_0^j \otimes \mathbf{a}_0^i\right) \quad (11)$$

With regard to a uni-axial loading test of a colonic wall specimen (Fig. 1*C–F*), let L, T and K be the loading, the transverse and the specimen thickness directions, respectively, which provide the orthogonal system LTK. The deformation gradient $\mathbf{F}$ can be assumed to be a diagonal tensor with principal stretches λ_L, λ_T and λ_K (Natali *et al.* 2009). If θ is the crossing angle that the collagen fibres of the submucosa form with the circumferential direction, and β is the angle between loading and circumferential directions, the unit vectors of the fibre families can be specified in the system LTK as follows (Fig. 1*C–F*):

$$\mathbf{a}_0^1 = [\cos\beta\cos\theta + \sin\beta\sin\theta,\ \sin\beta\cos\theta - \cos\beta\sin\theta,\ 0] \quad (12)$$

$$\mathbf{a}_0^2 = [\sin\beta\sin\theta - \cos\beta\cos\theta, -\sin\beta\cos\theta - \cos\beta\sin\theta,\ 0] \quad (13)$$

$$\mathbf{a}_0^3 = [\cos\beta, \sin\beta, 0] \quad (14)$$

where superscripts 1, 2 and 3 are associated to the two collagen fibre families of the submucosa and the muscular fibre family of the muscularis externa, respectively. Accounting for the deformation gradient assumed and the unit vectors of the fibre families, the specific formulations of nominal stress components can be evaluated (Natali *et al.* 2009).

Constitutive parameters are identified by comparing the model and experimental results. The comparison was performed accounting for the trends of both the nominal stress along the loading direction, P_{LL}, and the transverse stretch, λ_{T}, with the loading stretch, λ_{L}. The average experimental curves were adopted within the computation. The comparison of experimental and model results required a cost function to be provided, which evaluates the discrepancy between experimental data and model results, as follows:

$$\Omega(\omega) = \sum_{\beta=0^\circ,30^\circ,60^\circ,90^\circ}\left[\sqrt{\frac{1}{n^\beta}\sum_{z=1}^{n^\beta}\left(2-\frac{\left(P^{\mathrm{exp}}_{\mathrm{LL}\,z}\right)^\beta}{\left(P^{\mathrm{mod}}_{\mathrm{LL}\,z}\right)^\beta}-\frac{\left(P^{\mathrm{mod}}_{\mathrm{LL}\,z}\right)^\beta}{\left(P^{\mathrm{exp}}_{\mathrm{LL}\,z}\right)^\beta}\right)} + \sqrt{\frac{1}{n^\beta}\sum_{z=1}^{n^\beta}\left(2-\frac{\left(\lambda^{\mathrm{exp}}_{\mathrm{T}\,z}\right)^\beta}{\left(\lambda^{\mathrm{mod}}_{\mathrm{T}\,z}\right)^\beta}-\frac{\left(\lambda^{\mathrm{mod}}_{\mathrm{T}\,z}\right)^\beta}{\left(\lambda^{\mathrm{exp}}_{\mathrm{T}\,z}\right)^\beta}\right)}\right] \quad (15)$$

where superscript β specifies the loading direction, index z the specific experimental datum and n^β the number of experimental data, while superscripts 'exp' and 'mod' specify experimental and model results, respectively. The variable $\boldsymbol{\omega}$ represents the set of constitutive parameters, K_v, r, C_1 and α_1, which characterize the ground matrix, C_4^1, α_4^1, C_4^2, α_4^2 and C_{89}^{12} for submucosal collagen fibres and C_4^3 and α_4^3 for muscularis externa muscular fibres. Fibre helixes of the submucosa are characterized by the same mechanical configuration, and the same constitutive parameters were assumed, i.e. $C_4^1 = C_4^2$ and $\alpha_4^1 = \alpha_4^2$. The orientation of collagen fibres, as the angle θ, was assumed as a further parameter to be identified.

With regard to each experimental situation investigated, given the experimental values of tissue stretch along the loading direction, $\lambda_{\mathrm{L}}^{\mathrm{exp}}$, the model values $P_{\mathrm{LL}}^{\mathrm{mod}}$ and $\lambda_{\mathrm{T}}^{\mathrm{mod}}$ must be computed. The first Piola–Kirchhoff stress tensor, which is defined by eqns (7)–(11), depends on the principal invariants $\tilde{I}_1$, J, I_4^i, I_8^{ij} and I_9^{ij}, which, in turn, are functions of the principal stretches λ_{L}, λ_{T} and λ_{K}. Given the experimental stretch, $\lambda_{\mathrm{L}}^{\mathrm{exp}}$, the model values of the principal stretches $\lambda_{\mathrm{T}}^{\mathrm{mod}}$ and $\lambda_{\mathrm{K}}^{\mathrm{mod}}$ can be computed, accounting for the uni-axial configuration of experimental tests (Natali *et al.* 2007), as follows:

$$P_{\mathrm{TT}}\left(\lambda_{\mathrm{L}}^{\mathrm{exp}}, \lambda_{\mathrm{T}}^{\mathrm{mod}}, \lambda_{\mathrm{K}}^{\mathrm{mod}}\right) = 0,$$

$$P_{\mathrm{KK}}\left(\lambda_{\mathrm{L}}^{\mathrm{exp}}, \lambda_{\mathrm{T}}^{\mathrm{mod}}, \lambda_{\mathrm{K}}^{\mathrm{mod}}\right) = 0 \quad (16)$$

The solution of the algebraic non-linear system in eqn (16) leads to the stretch components $\lambda_{\mathrm{T}}^{\mathrm{mod}}$ and $\lambda_{\mathrm{K}}^{\mathrm{mod}}$ and makes it possible to evaluate the nominal stress, $P_{\mathrm{LL}}^{\mathrm{mod}} = P_{\mathrm{LL}}(\lambda_{\mathrm{L}}^{\mathrm{exp}}, \lambda_{\mathrm{T}}^{\mathrm{mod}}, \lambda_{\mathrm{K}}^{\mathrm{mod}})$.

The optimal set of constitutive parameters, ω^{opt}, was identified by minimizing the cost function, which was performed by specific optimization algorithms (Corana *et al.* 1987; Natali *et al.* 2009, 2011). The main challenge of the identification pertains to the uniqueness and the reliability of the parameters themselves. With regard to the uniqueness of parameters, the identification has to be performed accounting for independent experimental curves, i.e. the nominal stress–loading stretch or the transverse stretch–loading stretch data sets. The number of independent curves depends on the assumed set of parameters. To be precise, when five initial stiffness parameters, K_v,C_1, $C_4^1 = C_4^2$, C_4^3 and C_{89}^{12}, and one fibre distribution parameter, θ, together with the associated non-linearity parameters, r, α_1, $\alpha_4^1 = \alpha_4^2$ and α_4^3, have to be identified, at least six independent experimental curves have to be accounted for (Carniel *et al.* 2013*a*). The present study accounted for eight independent curves, i.e. four independent nominal stress–loading stretch data sets and four independent transverse stretch–loading stretch data sets.

Assessment of reliability of constitutive parameters

The reliability of the achieved parameters was assessed by the computation of model results for the experimental tests that were not accounted for within the identification of the parameters, using the results of the tensile tests along the 15 and 45 deg directions. Afterwards, model results were compared with experimental data.

A further check of the reliability of the parameters pertained to the evaluation of satisfaction of thermo-mechanics material stability requirements, as the polyconvexity of the strain energy function (Hartmann & Neff, 2003; Ehret & Itskov, 2007; Natali *et al.* 2009; Carniel *et al.* 2013*a*). When the analysis pertains to uni-axial loading conditions, the polyconvexity requirement can be checked by computation of the tangent Young modulus, which must show a convex trend with stretch, and the tangent Poisson ratios, which must be positive (Lempriere, 1968; Scott, 2007). According to the large strain field assumed, the tangent Young modulus, E_{L}, and the tangent Poisson ratios, ν_{LT} and ν_{LK}, are properly defined by the following formulations:

$$E_{\mathrm{L}} = \lambda_{\mathrm{L}}\frac{\mathrm{d}\sigma_{\mathrm{LL}}}{\mathrm{d}\lambda_{\mathrm{L}}} \quad (17)$$

$$\nu_{\mathrm{LT}} = -\frac{\mathrm{d}\ln\lambda_{\mathrm{T}}}{\mathrm{d}\ln\lambda_{\mathrm{L}}} = -\frac{\lambda_{\mathrm{L}}}{\lambda_{\mathrm{T}}}\frac{\mathrm{d}\lambda_{\mathrm{T}}}{\mathrm{d}\lambda_{\mathrm{L}}} \tag{18}$$

$$\nu_{\mathrm{LK}} = -\frac{\mathrm{d}\ln\lambda_{\mathrm{K}}}{\mathrm{d}\ln\lambda_{\mathrm{L}}} = -\frac{\lambda_{\mathrm{L}}}{\lambda_{\mathrm{K}}}\frac{\mathrm{d}\lambda_{\mathrm{K}}}{\mathrm{d}\lambda_{\mathrm{L}}} \tag{19}$$

where σ_{LL} is the true Cauchy stress that can be computed from the nominal stress P_{LL} according to standard push-forward operations (Holzapfel, 2000*b*), as $\sigma_{\mathrm{LL}} = \lambda_{\mathrm{L}} J^{-1} P_{\mathrm{LL}}$. The computation of E_{L}, ν_{LT} and ν_{LK} for a given value of stretch, λ_{L}, requires the knowledge of transverse stretches, λ_{T} and λ_{K}, and their first derivatives. Transverse stretches can be evaluated by solving the non-linear system, eqn (16), while the derivatives can be evaluated by the implicit function theorem (Krants & Parks, 2002; Natali *et al.* 2009), as follows:

$$\begin{bmatrix} \dfrac{\mathrm{d}\lambda_{\mathrm{T}}}{\mathrm{d}\lambda_{\mathrm{L}}} \\[2ex] \dfrac{\mathrm{d}\lambda_{\mathrm{K}}}{\mathrm{d}\lambda_{\mathrm{L}}} \end{bmatrix} = -\begin{bmatrix} \dfrac{\partial P_{22}}{\partial\lambda_{\mathrm{T}}} & \dfrac{\partial P_{22}}{\partial\lambda_{\mathrm{K}}} \\[2ex] \dfrac{\partial P_{33}}{\partial\lambda_{\mathrm{T}}} & \dfrac{\partial P_{33}}{\partial\lambda_{\mathrm{K}}} \end{bmatrix}^{-1} \begin{bmatrix} \dfrac{\partial P_{\mathrm{TT}}}{\partial\lambda_{\mathrm{L}}} \\[2ex] \dfrac{\partial P_{\mathrm{KK}}}{\partial\lambda_{\mathrm{L}}} \end{bmatrix} \tag{20}$$

Results

The data from the mechanical tests performed on colonic tissue specimens were postprocessed to provide averaged experimental curves within domains of reliable results. In Fig. 2, the tensile stress–stretch behaviour of colonic tissues is reported for the different directions investigated, i.e. 0, 15, 30, 45, 60 and 90 deg. In Fig. 3, a comparison of the mechanical response of the tissues along the different directions is shown. Averaged curves are shown for the trends in both the nominal stress (Fig. 3*A*) and the transverse stretch (Fig 3*B*) with the loading stretch. Averaged data are reported within supporting information.

The constitutive parameters of the proposed hyperelastic formulation were identified by analysis of the data from the mechanical tests. In detail, the evaluation of parameters was performed accounting for data from mechanical tests along 0, 30, 60 and 90 deg directions (Fig. 4). The following parameters were achieved: $K_v = 88.754$MPa, $r = 71.594$, $C_1 = 0.028$MPa and $\alpha_1 = 0.814$ for the ground matrix; $C_4^1 = C_4^2 = 0.039$MPa, $\alpha_4^1 = \alpha_4^2 = 0.107$, $C_{89}^{12} = 0.020$MPa and $\theta = 31.312$ degrees for collagen fibres of the submucosa; and $C_4^3 = 0.022$MPa and $\alpha_4^3 = 1.625$ for muscular fibres of the muscularis externa. The reliability of the parameters was assessed by analysis of the experimental tests along 15 and 45 deg directions, as shown in Fig. 5. The thermomechanical consistency of model and parameters was evaluated by the computation of tangent elastic moduli, i.e. the tangent Young modulus and tangent Poisson ratios. In detail, in Fig. 6 the trends of initial moduli, as the tangent moduli when the strain approaches zero, with the loading direction is reported for the Young modulus (Fig. 6*A*) and the Poisson ratios (Fig. 6*B*). The overall trend of the tangent Young modulus with both the loading direction and the loading stretch is reported in Fig. 6*C* and *D*.

Discussion

General discussion about methods and results

In this study, the constitutive analysis of colonic tissues was developed to provide a mathematical framework that interprets the specific biological tissue mechanics. The analysis was performed accounting for the histological investigation of the tissues to evaluate their structural configuration, experimental tests to provide the reference mechanical data and mathematical computations to define the constitutive model and to identify the associated parameters. The histological analysis showed the complex configuration of the colonic wall, as a structure that is composed of layers of different fibre-reinforced biological tissues. The fibres are aligned along three different preferential directions, suggesting a fully anisotropic behaviour. It followed that the planning of mechanical tests must account for different loading conditions along different directions. As a result of the typical tensile functionality of colonic tissues, mechanical tests were performed considering tensile conditions. The tests were developed according to six different loading directions. Experimental data were postprocessed to define averaged curves and reliable domains of experimental results (Figs 2 and 3), which agree with data previously provided by other authors (Egorov *et al.* 2002). The trends of both nominal stress and transverse stretch with the loading stretch were investigated. The constitutive formulation was provided accounting for the results from the histological investigation and the mechanical tests. In order to account for the composite configuration of the tissue and the non-linear geometric and material behaviour, a specific hyperelastic formulation was developed in the framework of fibre-reinforced composite materials theory. The model was defined starting from formulations that have already proved their reliability in analysis of the mechanics of soft biological tissues (Natali *et al.* 2009, 2010, 2011, 2012*a*,*b*). The constitutive parameters were evaluated by minimizing the discrepancy between model and experimental results, accounting for data from tensile tests performed along four directions. The data from tests performed along the remaining directions were analysed to assess the reliability of the parameters achieved. The capability of the proposed constitutive formulation to interpret the mechanics of colonic tissues is shown in Figs 4 and 5. The thermomechanical consistency of model and parameters was evaluated by computing the tangent Young modulus, which showed a convex trend with the loading stretch along all the loading directions, and the tangent Poisson ratios, which were always positive (Fig. 6). This configuration of parameters ensured satisfaction of the requirements of thermomechanics (Lempriere, 1968; Schröder *et al.* 2005).

Methodological considerations

The proposed constitutive analysis provides a procedure that should be adopted to perform the mechanical characterization of the different gastrointestinal tissues,

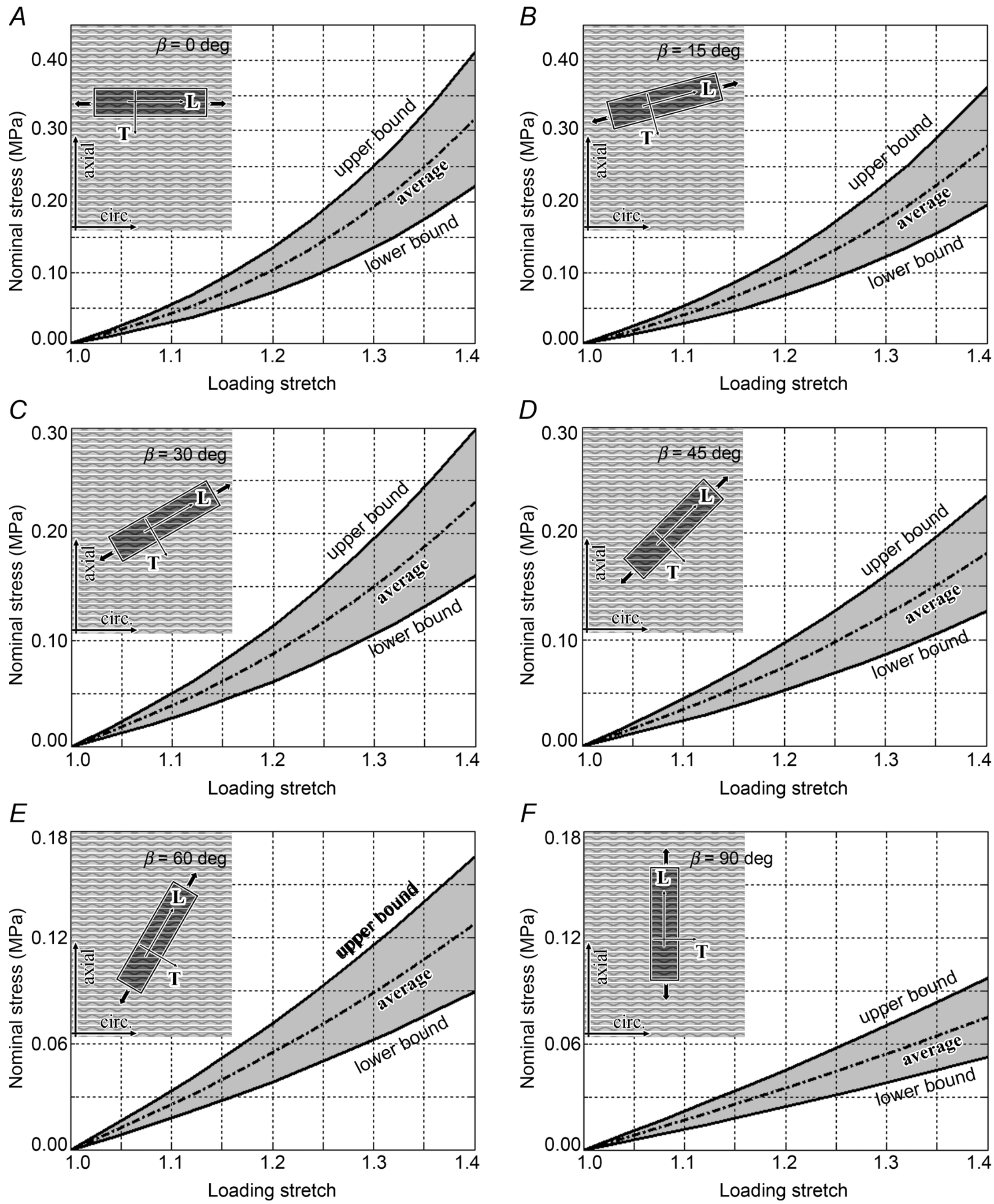

Figure 2. Experimental data from tensile tests performed along different directions, i.e. 0 (*A*), 15 (*B*), 30 (*C*), 45 (*D*), 60 (*E*) and 90 deg (*F*)
The average nominal stress–loading stretch curves are reported together with the domains of reliable experimental results. With regard to each loading direction, the localization of the specimen within the colonic wall is reported together with the stress–stretch data.

which is mandatory for the definition of computational models of gastrointestinal structures. The development of reliable computational models requires careful identification of the mechanical response of the biological tissues. This must be done by the definition of structurally coherent constitutive models, as formulations that account for the real configuration of the tissue, as the distribution of the different fibre families and their different contributions to the overall mechanical response. Different experimental tests and constitutive formulations have previously been proposed to characterize the mechanics of various tissues from different gastrointestinal organs, with regard to hyperelastic and visco-hyperelastic models (Goyal *et al.* 1971; Watters *et al.* 1985*a*,*b*; Egorov *et al.* 2002; Yang *et al.* 2006; Rose *et al.* 2008; Natali *et al.* 2009; Ciarletta *et al.* 2009; Bellini *et al.* 2011). The main deficiencies in these activities and formulations pertain to the loading situations that were investigated experimentally to provide the mechanical characterization of the tissues. Usually, mechanical tests were performed accounting for tensile and/or shear tests along circumferential and longitudinal directions and/or compression tests along wall thickness. Owing to the complex histological configuration, in particular with regard to the organization of the fibres, these loading conditions make it possible only partly to appreciate and identify the strongly anisotropic properties of gastrointestinal tissues. In contrast, the present approach accounts for the different fibre families by specific strain energy contributions, whose

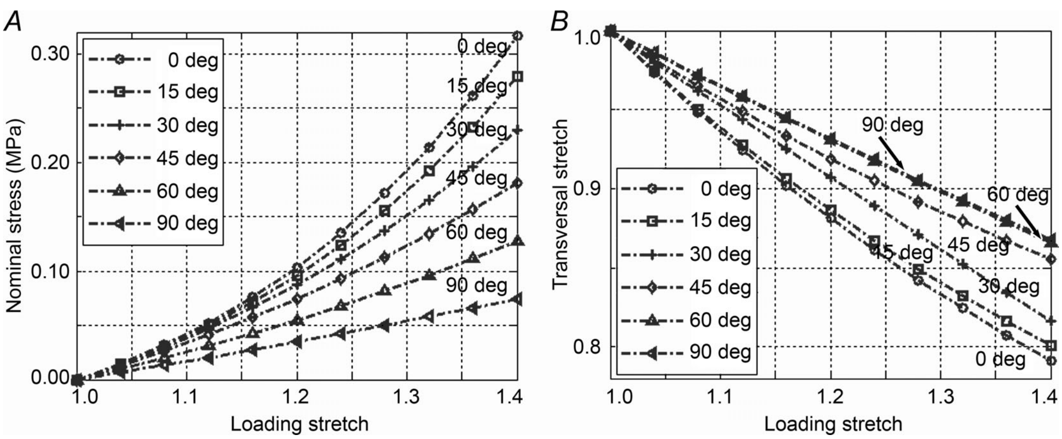

Figure 3. Comparison of mechanical behaviour of colonic tissues in the tensile tests performed along the different loading directions
A, average nominal stress–loading stretch curves. *B*, average transverse stretch–loading stretch curves.

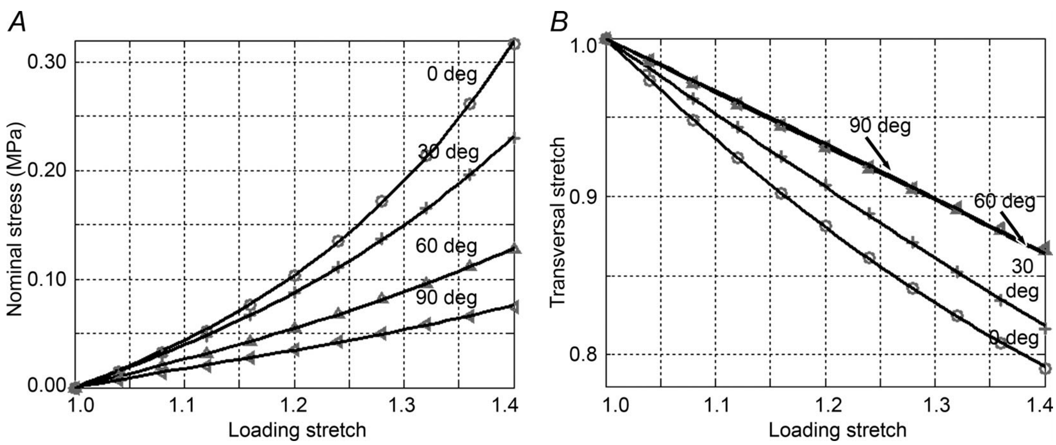

Figure 4. Evaluation of constitutive parameters by minimization of the discrepancy between model results and experimental data, accounting for tensile tests performed along 0 ($\Omega^{0^\circ} = 0.0028$), 30 ($\Omega^{30^\circ} = 0.0013$), 60 ($\Omega^{60^\circ} = 0.0018$) and 90 deg directions ($\Omega^{90^\circ} = 0.0023$)
Model results (continuous lines) and average experimental data (symbols) are reported for the trends of both nominal stress (*A*) and transverse stretch (*B*) with loading stretch.

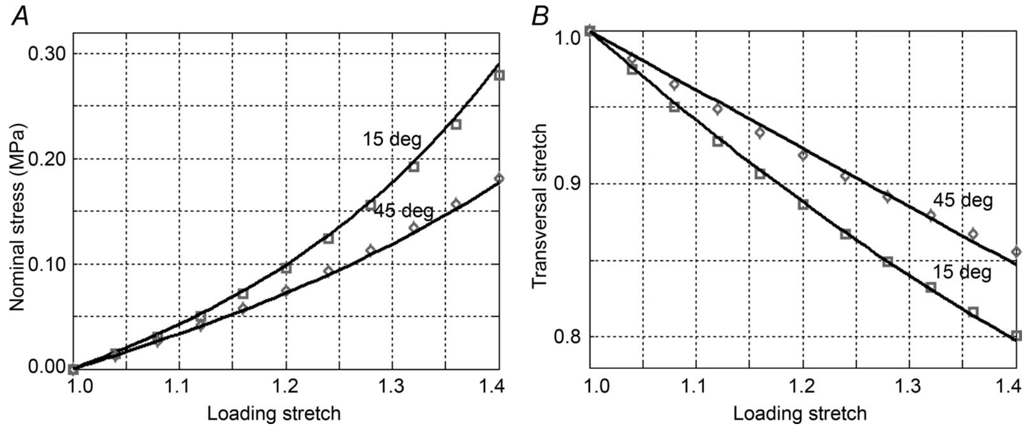

Figure 5. Assessment of the reliability of constitutive parameters by comparison of the model results and experimental data, accounting for tensile tests performed along 15 ($\Omega^{15^\circ} = 0.0047$) and 45 deg directions ($\Omega^{45^\circ} = 0.0042$)
Model results (continuous lines) and average experimental data (symbols) are reported for the trends of both nominal stress (*A*) and transverse stretch (*B*) with loading stretch.

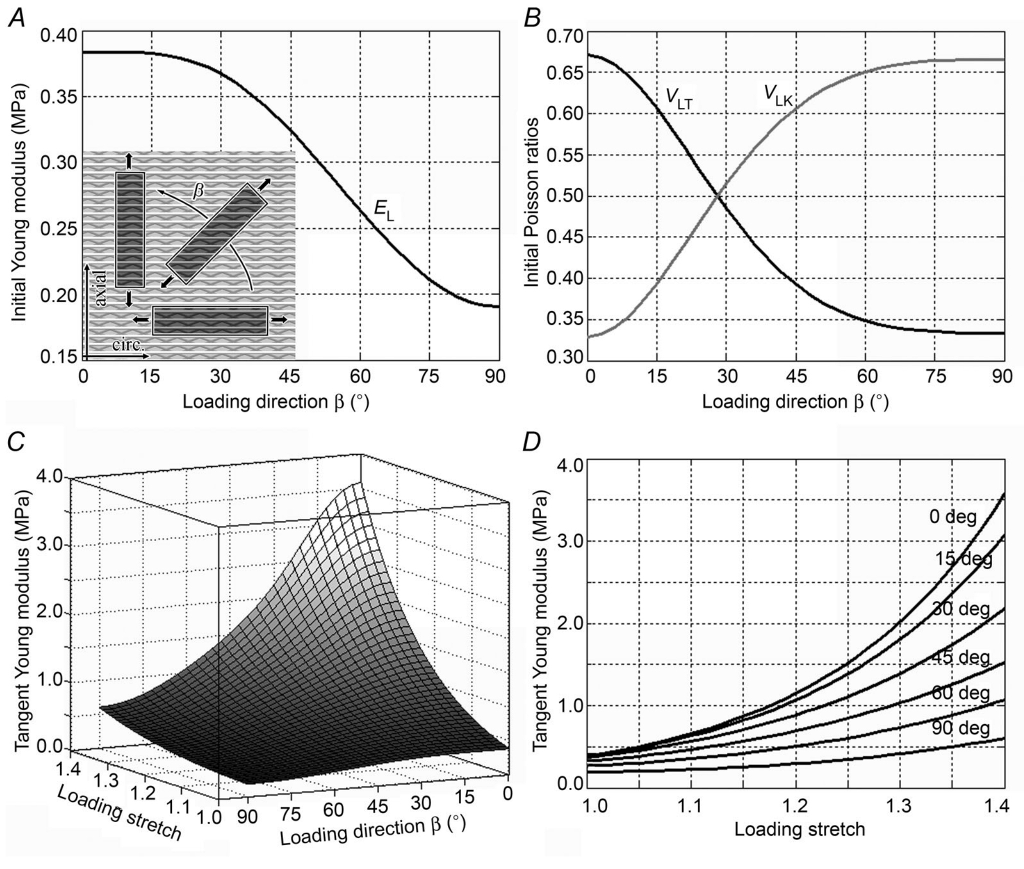

Figure 6. Evaluation of thermomechanical consistency of constitutive model and parameters
Trends of initial Young modulus (*A*) and initial Poisson ratios (*B*) with loading direction; and trends of tangent Young modulus with loading direction and loading stretch plotted as a surface (C) and as curves (*D*).

characterization and identification is performed by developing uni-axial tensile tests according to many different directions that are in agreement with the conformation of the fibres.

Limitations and future work

The main limitation of the present mechanical characterization pertains to damage of the connectivity of fibrous components resulting from preparation of the specimens. Furthermore, the cutting process modifies the prestressed configuration that characterizes the tissues *in situ* (Gregersen *et al.* 2000; Gregersen, 2003). With particular regard to tests developed along 0, 15, 30, 45 and 60 deg, an additional limitation of uni-axial tensile testing is due to flexural stresses that develop because of sample straightening. In other words, specimens cut along 0, 15, 30, 45 and 60 deg directions must be straightened before tensile testing. A straightening load must be applied and determines the flexural stresses. However, the straightening load is usually very much lower than the force values that are required to stretch the tissue samples during tensile testing, and the influence of flexural stresses is almost negligible. Nonetheless the reported limitations, tensile tests or other tests on specimens with simple geometry have been widely adopted to investigate the mechanical behaviour of biological tissues from the gastrointestinal tract or other tubular organs (Fung, 1993; Egorov *et al.* 2002; Gasser *et al.* 2006; Yang *et al.* 2006; Rosen *et al.* 2008; Ciarletta *et al.* 2009; Bellini *et al.* 2011; Carniel *et al.* 2014*a*). In fact, such tests provide information about tissue mechanics that are not otherwise achievable, such as the anisotropic conformation, stiffening phenomena with stretch, yielding, viscous and damage effects.

Accounting for the limitations of experimental tests on specimens with simple geometry, further experimentations are needed to assess and refine the constitutive framework. More detailed experimental tests should be performed without breaking the tissue and structure connectivity, and tests should be developed on tubular samples (i.e. inflation tests; Goyal *et al.* 1971; Hoeg *et al.* 2000; Carniel *et al.* 2013*a*, 2014*b*). Such experimental situations lead to complex stress and strain conditions within the biological tissues involved and do not properly highlight typical mechanical properties of the biological tissues, such as the anisotropic conformation. Consequently, experimental data from structural tests should not be applied to define the constitutive framework and to identify the constitutive parameters. The best approach to gastrointestinal tissue mechanics should account for many different experimental tests, including both tensile tests (or similar) and structural tests. Data from tensile tests must be processed to provide and identify the constitutive framework. Finite element models must be developed to interpret the structural tests; finally, numerical and experimental results must be compared to assess the reliability of the constitutive formulation and parameters.

A further topic of future investigation pertains to the dissipative phenomena, such as viscous and damage phenomena, which may develop when gastrointestinal tissues are stimulated mechanically. The analysis should provide a more comprehensive evaluation of the functionality of gastrointestinal tissues, with particular regard to degenerative situations. More refined constitutive formulations should be proposed to account for such phenomena. Although complex constitutive formulations, such as visco-hyperelastic (Pena *et al.* 2007; Natali *et al.* 2010; Rubini *et al.* 2011; Fontanella *et al.* 2012; Carniel *et al.* 2013*b*) and visco-hyperelasto-damage models (Natali *et al.* 2008; Pena *et al.* 2008), have been already provided for soft biological tissues, more experimental investigations are required for reliable application to the mechanics of the colon and gastrointestinal tissues in general.

References

Bellini C, Glass P, Sitti M & Di Martino ES (2011). Biaxial mechanical modeling of the small intestine. *J Mech Behav Biomed* **4**, 1727–1740.

Böhme J, Shim V, Höch A, Mütze M, Müller C & Josten C (2012). Clinical implementation of finite element models in pelvic ring surgery for prediction of implant behavior: a case report. *Clin Biomech* **27**, 872–878.

Carniel EL, Fontanella CG, Polese L, Merigliano S & Natali AN (2013*a*). Computational tools for the analysis of mechanical functionality of gastrointestinal structures. *Technol Health Care* **21**, 271–283.

Carniel EL, Fontanella CG, Stefanini C & Natali AN (2013*b*). A procedure for the computational investigation of stress relaxation phenomena. *Mech Time-Depend Mater* **17**, 25–38.

Carniel EL, Gramigna V, Fontanella CG, Stefanini C & Natali AN (2014*a*). Analysis of the passive mechanical behaviour of taeniae coli: experimental and numerical approach. *Journal of Mechanics in Medicine and Biology* **14**, 1–19, doi: 10.1142/S0219519414500122.

Carniel EL, Rubini A, Frigo A & Natali AN (2014*b*). Analysis of the biomechanical behaviour of gastrointestinal regions adopting an experimental and computational approach. *Comput Methods Programs Biomed* **113**, 338–345.

Ciarletta P, Dario P, Tendick F & Micera S (2009). Hyperelastic model of anisotropic fiber reinforcements within intestinal walls for applications in medical robotics. *Int J Robot Res* **28**, 1279–1288.

Corana A, Marchesi M, Martini C & Ridella S (1987). Minimizing multimodal functions of continuous variables with the Simulated Annealing algorithm. *ACM T Math Software* **13**, 262–280.

Egorov VI, Schastlivtsev IV, Prut EV, Baranov AO & Turusov RA (2002). Mechanical properties of the human gastrointestinal tract. *J Biomech* **35**, 1417–1425.

Ehret AE & Itskov M (2007). A polyconvex hyperelastic model for fiber-reinforced materials in application to soft tissues. *J Mater Sci* **42**, 8853–8863.

Fontanella CG, Matteoli S, Carniel EL, Wihljelm JE, Virga A, Corvi A & Natali AN (2012). Investigation on the load-displacement curves of a human healthy heel pad: *in vivo* compression data compared to numerical results. *Med Eng Phys* **34**, 1253–1259.

Forestiero A, Carniel EL & Natali AN (2014). Biomechanical behaviour of ankle ligaments: constitutive formulation and numerical modelling. *Comput Method Biomec* **17**, 395–404.

Fung YC (1993). *Biomechanics: Mechanical Properties of Living Tissues*, 2nd edn. Springer-Verlag, New York.

Gabella G (1987). The cross-ply arrangement of collagen fibres in the submucosa of the mammalian small intestine. *Cell Tissue Res* **248**, 491–497.

Gasser TC, Ogden RW & Holzapfel GA (2006). Hyperelastic modelling of arterial layers with distributed collagen fibre orientations. *J R Soc Interface* **3**, 15–35.

Ge Z, Schomacker KT & Nishioka NS (1998). Identification of colonic dysplasia and neoplasia by diffuse reflectance spectroscopy and pattern recognition techniques. *Appl Spectrosc* **52**, 833–839.

Goyal RK, Biancani P, Phillips A & Spiro HM (1971). Mechanical properties of the esophageal wall. *J Clin Invest* **50**, 1456–1465.

Gregersen H (2003). *Biomechanics of the Gastrointestinal Tract: New Perspectives in Motility Research and Diagnostics*. Springer-Verlag, London.

Gregersen H, Kassab GS & Fung YC (2000). The zero-stress state of the gastrointestinal tract. *Dig Dis Sci* **45**, 2271–2281.

Hartmann S & Neff P (2003). Polyconvexity of generalized polynomial-type hyperelastic strain energy functions for near-incompressibility. *Int J Solids Struct* **40**, 2767–2791.

Hidović-Rowe D & Claridge E (2005). Modelling and validation of spectral reflectance for the colon. *Phys Med Biol* **50**, 1071–1093.

Hoeg HD, Slatkin AB, Burdick JW & Grundfest WS (2000). Biomechanical modeling of the small intestine as required for the design and operation of a robotic endoscope. *P IEEE Int Conf Robot* **2**, 1599–1606.

Holzapfel GA (2000*a*). Biomechanics of soft tissues. In *Handbook of Material Behaviour: Non Linear Models and Properties*, ed. Lemaitre J, pp. 1057–1071. Academic Press LMT, Cachan.

Holzapfel GA (2000*b*). *Nonlinear Solid Mechanics*. Wiley, New York.

Huang Z, Zheng W, Xie S, Chen R, Zeng H, McLean DI & Lui H (2004). Laser-induced autofluorescence microscopy of normal and tumor human colonic tissue. *Int J Oncol* **24**, 59–63.

Hung PC & Voloshin AS (2003). In-plane strain measurement by digital image correlation. *J Braz Soc Mech Sci & Eng* **25**, 215–221.

Junqueira LC, Carneiro J & Long JA (2005). *Basic Histology*, 11th edn. McGraw-Hill Medical Publishing, New York.

Krantz SG & Parks HR (2002). *The Implicit Function Theorem: History, Theory and Applications*. Birkhäuser, Boston.

Lapeer RJ, Gasson PD & Karri V (2010). Simulating plastic surgery: from human skin tensile tests, through hyperelastic finite element models to real-time haptics. *Prog Biophys Mol Biol* **103**, 208–216.

Lempriere BM (1968). Poisson's ratio in orthotropic materials. *AIAA J* **6**, 2226–2227.

Liao DH, Zhao JB & Gregersen H (2009). Gastrointestinal tract modelling in health and disease. *World J Gastroenterol* **15**, 169–176.

Maurel W, Wu Y, Magnenat Thalmann N & Thalmann D (1998). *Biomechanical Models for Soft Tissue Simulation*. Springer, Berlin.

Natali AN, Carniel EL & Gregersen H (2009). Biomechanical behaviour of oesophageal tissues: material and structural configuration, experimental data and constitutive analysis. *Med Eng Phys* **31**, 1056–1062.

Natali AN, Carniel EL, Pavan PG, Bourauel C, Ziegler A & Keilig L (2007). Experimental–numerical analysis of minipig's multi-rooted teeth. *J Biomech* **40**, 1701–1708.

Natali AN, Carniel EL, Pavan PG, Sander FG, Dorow C & Geiger M (2008). A visco-hyperelastic-damage constitutive model for the analysis of the biomechanical response of the periodontal ligament. *J Biomech Eng* **130**, 031004.

Natali AN, Fontanella CG & Carniel EL (2010). Constitutive formulation and analysis of heel pad tissues mechanics. *Med Eng Phys* **32**, 516–522.

Natali AN, Fontanella CG & Carniel EL (2012*a*). A numerical model for investigating the mechanics of calcaneal fat pad region. *J Mech Behav Biomed* **5**, 216–223.

Natali AN, Fontanella CG & Carniel EL (2012*b*). Constitutive formulation and numerical analysis of the heel pad region. *Comput Methods Biomech Biomed Engin* **15**, 401–409.

Natali AN, Fontanella CG, Carniel EL & Miller-Young J (2011). Biomechanical behavior of heel pad tissues: experimental testing, constitutive formulation and numerical modeling. *Proc Inst Mech Eng H* **225**, 449–459.

Nováček V, Trần TN, Klinge U, Tolba RH, Staat M, Bronson DG, Miesse AM, Whiffen J & Turquier F (2012). Finite element modelling of stapled colorectal end-to-end anastomosis: advantages of variable height stapler design. *J Biomech* **45**, 2693–2697.

Owida AA, Do H & Morsi YS (2012). Numerical analysis of coronary artery bypass grafts: an overview. *Comput Methods Programs Biomed* **108**, 689–705.

Pena E, Calvo B, Martinez MA & Doblaré M (2007). An anisotropic visco-hyperelastic model for ligaments at finite strains. Formulation and computational aspects. *Int J Solids Struct* **44**, 760–778.

Pena E, Calvo B, Martinez MA & Doblaré M (2008). On finite-strain damage of viscoelastic-fibred materials. Application to soft biological tissues. *Int J Numer Meth Eng* **74**, 1198–1218.

Rosen J, Brown JD, De S, Sinanan M & Hannaford B (2008). Biomechanical properties of abdominal organs in vivo and postmortem under compression loads. *J Biomech Eng* **130**, 021020.

Ross MH, Romrell LJ & Kaye GI (2010). *Histology: a Text and Atlas*, 6th edn. Lippincott Williams & Wilkins, Philadelphia, PA, USA.

Rubini A, Carniel EL, Parmagnani A & Natali AN (2011). Flow and volume dependence of rat airway resistance during constant flow inflation and deflation. *Lung* **189**, 511–518.

Schröder J, Neff P & Balzani D (2005). A variational approach for materially stable anisotropic hyperelasticity. *Int J Solids Struct* **42**, 4352–4371.

Scott NH (2007). The incremental bulk modulus, Young's modulus and Poisson's ratio in nonlinear isotropic elasticity: physically reasonable response. *Math Mech Solids* **12**, 526–542.

Shrive NG (1996). Soft tissue strain measurements. In *Optical Measurement Methods in Biomechanics*, ed. Orr JF & Shelton JC, p. 154–172. Springer, London, UK.

Skinner SA & O'Brien PE (1996). The microvascular structure of the normal colon in rats and humans. *J Surg Res* **61**, 482–490.

Spencer AJM (1984). *Continuum Theory of the Mechanics of Fibre-Reinforced Composites*. Springer-Verlag, New York.

Tillier Y, Paccini A, Durand-Reville M, Bay F & Chenot J-L (2003). Three-dimensional finite element modelling for soft tissues surgery. *Int Congr Ser* **1256**, 349–355.

Watters DA, Smith AN, Eastwood MA, Anderson KC & Elton RA (1985*a*). Mechanical properties of the rat colon: the effect of age, sex and different conditions of storage. *Q J Exp Physiol* **70**, 151–162.

Watters DA, Smith AN, Eastwood MA, Anderson KC, Elton RA & Mugerwa JW (1985*b*). Mechanical properties of the colon: comparison of the features of the African and European colon *in vitro*. *Gut* **26**, 384–392.

Weiss JA & Gardiner JC (2001). Computational modeling of ligament mechanics. *Crit Rev Biomed Eng* **29**, 1–70.

Yang W, Fung TC, Chian KS & Chong CK (2006). 3D Mechanical properties of the layered esophagus: experiment and constitutive model. *J Biomech Eng* **128**, 899–908.

Additional Information

Competing interests

None declared.

Author contributions

E.L.C. conceived and designed the experimental tests. V.G. and C.S. provided the experimental samples and developed the experimental tests. E.L.C., C.G.F. and A.F. developed the constitutive formulation and the identification of parameters. A.R. revised the experimental testing procedures and the article. A.N.N. revised the overall research activities and the article. All authors approved the final version for publication.

Funding

None.

Supporting Information

The following supporting information is available in the online version of this article.

Averaged experimental data from tensile tests